Available online at www.sciencedirect.com
ScienceDirect
Nuclear Physics B 938 (2019) 131–142
www.elsevier.com/locate/nuclphysb

Contributions of vector leptoquark to $\Xi_b \to \Xi_c \tau \bar{\nu}_\tau$ decay

Jiao Zhang [a,*], Jianfeng Su [a], Qingguo Zeng [b]

[a] *Luoyang Institute of Science and Technology, Luoyang 471000, China*
[b] *Department of Physics, Shangqiu Normal University, Shangqiu 476000, China*

Received 31 May 2018; received in revised form 5 November 2018; accepted 13 November 2018
Available online 15 November 2018
Editor: Tommy Ohlsson

Abstract

Motivated by the $R_D^{(*)}$ anomalies in semileptonic B meson decay which can be explained by adding a single vector leptoquark $U_3(3, 3, \frac{2}{3})$ to the Standard Model, we further analyse the New Physics effects of vector leptoquark to the heavy baryon $\Xi_b \to \Xi_c \tau^- \bar{\nu}_\tau$ decay. Using the best-fit solutions for Wilson coefficients of operators resulted from experimental measurement $R_D^{(*)}$ anomalies and the form factors resulted from relativistic quark model, we study the contributions of the leptoquark to several observables, such as differential branching ratio, ratio of differential branching ratio, lepton-side forward-backward asymmetry, longitudinal polarization fraction of Ξ_c baryon and τ lepton as well as the convexity parameter of this decay with the helicity amplitude formalism. We find that the contributions of vector leptoquark to differential branching ratio, ratio of differential branching ratio and convexity parameter are significant which show deviations at high level from the corresponding Standard Model predictions. Nevertheless, the observables lepton-side forward-backward asymmetry, longitudinal polarization fraction of Ξ_c baryon and τ lepton have the same behaviours in vector leptoquark as that in the Standard Model which displays the three observables are not sensitive to the New Physics effects of vector leptoquark.

* Corresponding author.
E-mail address: zhangjiao198746@163.com (J. Zhang).

https://doi.org/10.1016/j.nuclphysb.2018.11.006

1. Introduction

The effects of lepton flavour universality violation (LFUV) have been observed in rare B meson semileptonic decays which may imply the indirect hints for New Physics (NP) in the flavour sector. In particular, the deviations between the experimental measurements for the ratios of charged current $b \to c l \bar{\nu}_\tau$ decays as well as neutral current $b \to s l \bar{l}$ decays and their Standard Model (SM) predictions, respectively. For the ratios $R_D^{(*)} = \frac{Br(B\to R_D^{(*)}\tau^-\bar{\nu}_\tau)}{Br(B\to R_D^{(*)}l^-\bar{\nu}_l)}$, with $l = e, \mu$ have been measured by BaBar [1,2], Bell [3–5] and LHCb [6,7] collaborations. These measurements provide the average ratios [8]:

$$
\begin{aligned}
R_D &= 0.407 \pm 0.039 \pm 0.024, \\
R_D^* &= 0.304 \pm 0.013 \pm 0.007,
\end{aligned}
\tag{1}
$$

which reveal significant deviations at 1.9σ and 3.3σ level from their relevant SM predictions, respectively. Similarly, another significant deviations from the SM prediction have also been reported for the ratios of $R_K^{(*)} = \frac{Br(B\to K^{(*)}\mu^+\mu^-)}{Br(B\to K^{(*)}e^+e^-)}$ [9,10]:

$$
\begin{aligned}
R_K &= 0.745^{+0.090}_{-0.074} \pm 0.036 \qquad && q^2 \in [1, 6]\ \mathrm{GeV}^2, \\
R^*_{K(low)} &= 0.66^{+0.11}_{-0.07} \pm 0.03 && q^2 \in [0.045, 1.1]\ \mathrm{GeV}^2, \\
R^*_{K(high)} &= 0.69^{+0.11}_{-0.07} \pm 0.05 && q^2 \in [1.1, 6]\ \mathrm{GeV}^2,
\end{aligned}
\tag{2}
$$

which deviate from their SM predictions at 2.6σ, 2.1σ and 2.4σ level, correspondingly. Recently, LHCb reported a new anomaly about ratio [11]:

$$
R_{J/\Psi} = \frac{Br(B^+ \to J/\Psi\tau^+\nu_\tau)}{Br(B^+ \to J/\Psi\mu^+\mu_\tau)} = 0.71 \pm 0.17 \pm 0.18,
\tag{3}
$$

which deviates from the SM prediction at more than 2σ level [12,13], although the error are too large at present to reach a definitive conclusion.

The deviations between the experimental measurements $R_D^{(*)}$ and SM predictions have attracted a great deal of attention in the particle physics and many theoretical studies have been done to look for the explanation in different NP models, among which Ref. [14] has resolved the anomalies through adding a single vector leptoquark (LQ) transforming as $(3, 3, \frac{2}{3})$ to the SM. Combining the constraints from the experimental measurements of $R_D^{(*)}$ anomalies and the contributions of vector LQ to $B \to D^{(*)}\tau\bar{\nu}_\tau$ decays, the two best-fit solutions denoted as R_A and R_B for the Wilson coefficients of operators are given in Ref. [15]. Additional, NP effects of $R_D^{(*)}$ anomalies on $\Lambda_b \to \Lambda_c l \bar{\nu}_l$ decays [16–21] and $B \to J/\Psi l \bar{\nu}_l$ decays [13,22–24] have been researched. The weak and semileptonic decay of heavy baryons are very important not only in obtaining information about their internal structure, precise calculation of the main ingredients of SM such as Cabibbo–Kobayashi–Maskawa (CKM) matrix elements and answering to some fundamental questions like nature of the CP violation, but also in looking for NP beyond the SM [25]. Inspired by these advantages of baryon semileptonic decays as well as the works about explanations for $R_D^{(*)}$ anomalies and NP effects on analogous $b \to c l \bar{\nu}_l$ decays, we further study the heavy baryon decay $\Xi_b \to \Xi_c \tau \bar{\nu}_\tau$ using the helicity amplitude formalism and the form factors resulted from relativistic quark model within the SM explored with a single vector leptoquark (LQ) which can successfully resolve the $R_D^{(*)}$ anomalies. Many works have been done for $\Xi_b \to \Xi_c l \bar{\nu}_l$ decays [26–32]. The NP effects of scalar LQ to the heavy baryon semileptonic $\Xi_b \to \Xi l \bar{l}$ also have been researched in Ref. [33]. Ref. [32] has discussed the NP effects of vector and scalar type contributions to this transition in the model independent way. Nevertheless, we decide to study this decay in a specific vector LQ $U_3(3, 3, \frac{2}{3})$ model. In this case, the numerical results depend on not only the couplings between LQ and quarks(leptons), but also the mass of the LQ. We report the contributions of vector LQ to several observables, such as differential branching ratio $DBR(q^2)$, ratio of differential branching ratio $R_{\Xi_c}(q^2)$, lepton-side forward-backward asymmetry $A_{FB}(q^2)$, longitudinal polarization fraction of Ξ_c baryon $P_{\Xi_c}(q^2)$ and τ lepton $P_\tau(q^2)$ as well as the convexity parameter $C_F(q^2)$ relevant to this decay and contrast our results with SM predictions. It should be taken notice that we introduce additional observable $P_{\Xi_c}(q^2)$ which is absent in Ref. [32]. The observable $R_{\Xi_c}(q^2)$ is so important that we hope it will be detected on high energy collider in the future. Once it is measured, this could be recognized as the continuity of NP effects implied in $R_D^{(*)}$ which may further clarify the existence of NP. All of these observables are q^2 dependent which will be introduced in detail within the section 3.

The paper is organized as follows. In section 2, we briefly introduce the SM extended by a vector LQ $U_3(3, 3, \frac{2}{3})$ which can generate purely left-handed current with quarks and leptons. In section 3, we give the helicity amplitudes and introduce several observables for the baryon semileptonic $\Xi_b \to \Xi_c \tau \bar{\nu}_\tau$ decay. In section 4, the contributions of vector LQ to the several observables $DBR(q^2)$, $R_{\Xi_c}(q^2)$, $A_{FB}(q^2)$, $P_{\Xi_c}(q^2)$, $P_\tau(q^2)$ and $C_F(q^2)$ are reported. Finally, we give the conclusion in section 5.

2. The vector LQ $U_3(3, 3, \frac{2}{3})$

Ref. [14] has extended the SM by a vector $SU(2)_L$ triplet LQ generating purely left-handed currents with quarks and leptons which can successfully resolve the $R_D^{(*)}$ anomalies. The vector triplet U_3^μ having the charge arrangement $(3, 3, \frac{2}{3})$ under the SM gauge group couples to a leptoquark current with (V–A) structure:

$$\mathcal{L} = g_{ij} \bar{Q}_i \gamma^\mu \tau^A U^A_{3\mu} L_j + h.c., \tag{4}$$

where τ^A $(A = 1, 2, 3)$ are the Pauli matrices in the $SU(2)_L$ space, and Q_i and L_j $(i, j = 1, 2, 3$ generation) indicate the quarks and left-handed leptons $SU(2)_L$ doublet, respectively. For simplicity, g_{ij} is real and defined as the couplings of the $Q = 2/3$ component of the triplet, $U^{2/3}_{3\mu}$, to $\bar{d}_{Li}$ and l_{Lj}. Expending other $SU(2)_L$ components $U^{5/3}_{3\mu}$ and $U^{-1/3}_{3\mu}$, the Lagrangian Eq. (4) written in mass basis changes to eigencharge state as:

$$\begin{aligned}\mathcal{L}_{U3} = {} & U^{2/3}_{3\mu} \left[(\mathcal{V} g \mathcal{U})_{ij}\, \bar{u}_i \gamma^\mu P_L \nu_j - g_{ij} \bar{d}_i \gamma^\mu P_L l_j \right] \\ & + U^{5/3}_{3\mu} (\sqrt{2} \mathcal{V} g)_{ij} \bar{u}_i \gamma^\mu P_L l j \\ & + U^{-1/3}_{3\mu} (\sqrt{2} g \mathcal{U})_{ij} \bar{d}_i \gamma^\mu P_L \nu_j + h.c.,\end{aligned} \tag{5}$$

where $\mathcal{V}$ denotes the CKM matrix and $\mathcal{U}$ denotes the PontecorvoMaki–Nakagawa–Sakata (PMNS) matrix.

The semileptonic decay $b \to c\tau\bar{\nu}_\tau$ proceed via exchange of vector multiplet U_3^μ at three level. Combining the SM contribution and LQ correction, the effective weak Hamiltonian is written as [14]

$$H_{eff} = \frac{2G_F V_{cb}}{\sqrt{2}}[C_V(\bar{\tau}\gamma_\mu P_L \nu_\tau)(\bar{c}\gamma^\mu b) - C_A(\bar{\tau}\gamma_\mu P_L \nu_\tau)(\bar{c}\gamma^\mu \gamma_5 b)], \tag{6}$$

where C_V and C_A represent the Wilson coefficients for both SM and NP contributions of the operators coming from vector and pseudo-vector type of interactions, respectively. At the matching scale $\mu = M_U$, they are written as:

$$C_V = C_A = 1 + \frac{\sqrt{2} g^*_{b\tau}(\mathcal{V}g)_{c\tau}}{2G_F V_{cb} M_U^2}, \tag{7}$$

where we can see that the vector LQ only generates (V–A) couplings.

Direct searches for LQs have pushed model independent lower limits on their masses up to a TeV scale. Taking into account the constraints on the vector LQ mass by CMS collaboration [34,35], in our numerical results, we assume that the mass of vector LQ M_U is 1 TeV. The vector LQ U_3^μ could explain the $R_D^{(*)}$ and $R_K^{(*)}$ simultaneously [14]. Although $R_D^{(*)}$ anomalies also can be explained by mediating W', ATLAS [36] and CMS [37] have already constrained the W' mass down to 500 GeV and 300 GeV, respectively. Ref. [38] has the conclusion that the mass range $250 \sim 700$ GeV for W' can be probed at 5σ level with special values of couplings. We can see that the collider research limits for masses of LQ and W' is distinguished. Fitting to the measurement results of $R_D^{(*)}$ and accompanying the acceptable q^2 spectra, two best-fit solutions R_A and R_B are resulted in this scenario [15]:

$$g^*_{b\tau}(\mathcal{V}g)_{c\tau} = \begin{cases} 0.18 \pm 0.04 & R_A \\ -2.88 \pm 0.04 & R_B, \end{cases}$$

where we take $M_U = 1$TeV as a benchmark in the calculation.

3. Form factors and observables for $\Xi_b \to \Xi_c \tau \bar{\nu}_\tau$ decay

3.1. Form factors

Before computing the observables of $\Xi_b \to \Xi_c \tau\bar{\nu}_\tau$ transition mode, we need to parametrize the hadronic matrix elements of the vector and axial vector currents between the two spin half baryons. Hadronic matrix elements parametrized in form of various form factors can be written as [20,21]:

$$\begin{aligned}
\langle \Xi_c, \lambda_2 | V^\mu | \Xi_b, \lambda_1 \rangle &= \bar{u}_{\Xi_c}(p_2, \lambda_2)[f_1(q^2)\gamma_\mu + i f_2(q^2)\sigma_{\mu\nu}q^\nu + f_3(q^2)q_\mu] u_{\Xi_b}(p_1, \lambda_1), \\
\langle \Xi_c, \lambda_2 | A^\mu | \Xi_b, \lambda_1 \rangle &= \bar{u}_{\Xi_c}(p_2, \lambda_2)[g_1(q^2)\gamma_\mu + i g_2(q^2)\sigma_{\mu\nu}q^\nu + g_3(q^2)q_\mu]\gamma_5 u_{\Xi_b}(p_1, \lambda_1),
\end{aligned} \tag{8}$$

where $q = p_1 - p_2$, $\sigma_{\mu\nu} = \frac{i}{2}(\gamma_\mu\gamma_\nu - \gamma_\nu\gamma_\mu)$, λ_1 and λ_2 denote the helicity of Ξ_b and Ξ_c baryons, respectively. It is convenient to parametrize the hadronic matrix elements in terms of four-vector velocities v^μ and v'^μ when both baryons are heavy,

$$\langle \Xi_c, \lambda_2 | V^\mu | \Xi_b, \lambda_1 \rangle = \bar{u}_{\Xi_c}(p_2, \lambda_2)[F_1(\omega)\gamma_\mu + F_2(\omega)v_\mu + F_3(\omega)v'_\mu]u_{\Xi_b}(p_1, \lambda_1),$$
$$\langle \Xi_c, \lambda_2 | V^\mu | \Xi_b, \lambda_1 \rangle = \bar{u}_{\Xi_c}(p_2, \lambda_2)[G_1(\omega)\gamma_\mu + G_2(\omega)v_\mu + G_3(\omega)v'_\mu]\gamma_5 u_{\Xi_b}(p_1, \lambda_1),$$
$$\omega = v \cdot v' = \frac{m_1^2 + m_2^2 - q^2}{2m_1 m_2}, \tag{9}$$

where m_1 and m_2 represent the mass of Ξ_b and Ξ_c baryons, respectively. The relationship between two sets of form factors can be expressed as the follows [32]:

$$f_1(q^2) = F_1(q^2) + (m_1 + m_2)\left[\frac{F_2(q^2)}{2m_1} + \frac{F_3(q^2)}{2m_2}\right],$$
$$f_2(q^2) = \frac{F_2(q^2)}{2m_1} + \frac{F_3(q^2)}{2m_2},$$
$$f_3(q^2) = \frac{F_2(q^2)}{2m_1} - \frac{F_3(q^2)}{2m_2},$$
$$g_1(q^2) = G_1(q^2) - -(m_2 - m_1)\left[\frac{G_2(q^2)}{2m_1} + \frac{G_3(q^2)}{2m_2}\right],$$
$$g_2(q^2) = \frac{G_2(q^2)}{2m_1} + \frac{G_3(q^2)}{2m_2},$$
$$g_3(q^2) = \frac{G_2(q^2)}{2m_1} - \frac{G_3(q^2)}{2m_2}. \tag{10}$$

We use the form factors resulting from relativistic quark model which have been shown more explicitly in Ref. [26]. The equations related to our calculation are:

$$F_1(\omega) = \zeta(\omega) + \left(\frac{\bar{\Lambda}}{2m_b} + \frac{\bar{\Lambda}}{2m_c}\right)[2\chi(\omega) + \zeta(\omega)],$$
$$G_1(\omega) = \zeta(\omega) + \left(\frac{\bar{\Lambda}}{2m_b} + \frac{\bar{\Lambda}}{2m_c}\right)\left[2\chi(\omega) + \frac{\omega - 1}{\omega + 1}\zeta(\omega)\right],$$
$$F_2(\omega) = G_2(\omega) = -\frac{\bar{\Lambda}}{2m_c}\frac{2}{\omega + 1}\zeta(\omega),$$
$$F_3(\omega) = -G_3(\omega) = -\frac{\bar{\Lambda}}{2m_b}\frac{2}{\omega + 1}\zeta(\omega), \tag{11}$$

where $\bar{\Lambda} = m_1 - m_b$ is the difference of Ξ_b baryon and the heavy quark mass in the infinitely heavy quark limit $m_b \to \infty$. $\zeta(\omega)$ is the leading order Isgur-wise function and additional function $\chi(\omega)$ appeared for the sake of the kinetic energy term in $1/m_b$ correction to the heavy quark effective theory (HQET) Lagrangian. Near the zero recoil point of the final baryon $\omega = 1$, these functions can be approximated by

$$\zeta(\omega) = 1 - \rho_\zeta^2(\omega - 1) + c_\zeta(\omega - 1)^2,$$
$$\chi(\omega) = \rho_\chi^2(\omega - 1) + c_\chi(\omega - 1)^2, \tag{12}$$

where $\rho_\zeta^2 = -[d\zeta(\omega)/d\omega]_{\omega=1}$ is the solpe and $2c_\zeta = [d^2\zeta(\omega)/d^2\omega]_{\omega=1}$ is the curvature of the Isgur-wise function. All of these parameters will be given numerical values in the next section.

3.2. Observables

We now need to introduce the helicity amplitudes which have been defined by Refs. [17,21]

$$H^{V(A)}_{\lambda_2,\lambda_W} = \epsilon^{\dagger\mu}(\lambda_W)\langle\Xi_c,\lambda_2|V(A)^\mu|\Xi_b,\lambda_1\rangle,$$
$$H_{\lambda_2,\lambda_W} = H^V_{\lambda_2,\lambda_W} - H^A_{\lambda_2,\lambda_W}, \tag{13}$$

where λ_2 and λ_W denote the helicity of the Ξ_c baryon and $W^-_{\text{off-shell}}$, respectively. The helicity amplitudes can be written in form of form factors and the NP couplings as follows:

$$H^V_{1/2,0} = C_V\frac{\sqrt{(m_1-m_2)^2-q^2}}{\sqrt{q^2}}[(m_1+m_2)f_1(q^2)-q^2f_2(q^2)],$$
$$H^A_{1/2,0} = C_A\frac{\sqrt{(m_1+m_2)^2-q^2}}{\sqrt{q^2}}[(m_1-m_2)g_1(q^2)+q^2g_2(q^2)],$$
$$H^V_{1/2,1} = C_V\sqrt{2[(m_1-m_2)^2-q^2]}[-f_1(q^2)+(m_1+m_2)f_2(q^2)],$$
$$H^A_{1/2,1} = C_A\sqrt{2[(m_1+m_2)^2-q^2]}[-g_1(q^2)--(m_1-m_2)g_2(q^2)],$$
$$H^V_{1/2,t} = C_V\frac{\sqrt{(m_1+m_2)^2-q^2}}{\sqrt{q^2}}[(m_1-m_2)f_1(q^2)+q^2f_3(q^2)],$$
$$H^A_{1/2,t} = C_A\frac{\sqrt{(m_1-m_2)^2-q^2}}{\sqrt{q^2}}[(m_1+m_2)g_1(q^2)-q^2g_3(q^2)],$$
$$H^V_{\lambda_2,\lambda_W} = H^V_{-\lambda_2,-\lambda_W},$$
$$H^A_{\lambda_2,\lambda_W} = -H^A_{-\lambda_2,-\lambda_W}. \tag{14}$$

The differential angular distributions for $\Xi_b \to \Xi_c l\bar{\nu}_l$ decay can be written as [17,21]

$$\frac{d\Gamma(\Xi_b\to\Xi_c l\bar{\nu}_l)}{dq^2 d\cos\theta_l} = \frac{G_F^2|V_{cb}|^2q^2|\vec{p}_{\Xi_c}|}{512\pi^3m_1^2}\left(1-\frac{m_l^2}{q^2}\right)^2\left[A_1+\frac{m_l^2}{q^2}A_2\right], \tag{15}$$

with

$$A_1 = 2\sin^2\theta_l(H^2_{1/2,0}+H^2_{-1/2,0})+(1-\cos\theta_l)^2H^2_{1/2,1}+(1+\cos\theta_l)^2H^2_{-1/2,-1},$$
$$A_2 = 2\cos^2\theta_l(H^2_{1/2,0}+H^2_{-1/2,0})+\sin^2\theta_l(H^2_{1/2,1}+H^2_{-1/2,-1})+2(H^2_{1/2,t}+H^2_{-1/2,t})$$
$$-4\cos\theta_l(H_{1/2,t}H_{1/2,0}+H_{-1/2,t}H_{-1/2,0}),$$
$$|\vec{p}_{\Xi_c}| = \frac{\sqrt{(m_1^2)^2+(m_2^2)^2+(q^2)^2-2(m_1^2m_2^2+m_2^2q^2+m_1^2q^2)}}{2m_1}, \tag{16}$$

where $|\vec{p}_{\Xi_c}|$ is the momentum of the baryon Ξ_c and θ_l denotes the angle between the outgoing baryon Ξ_c and the lepton three momentum vector in the q^2 rest frame. We can easily perceive that the vector LQ only generates (V–A) couplings from Eq. (4) and (5). There is only vector type operator but no scalar or tensor operators in the contributions of vector LQ so that only the vector type contributions are concluded in these expressions.

Then we can obtain the q^2 dependent $DBR(q^2)$ by integrating out $\cos\theta_l$ from Eq. (15), i.e.,

$$DBR(q^2) = \left(\int_{-1}^{1} \frac{d\Gamma(\Xi_b \to \Xi_c l \bar{\nu}_l)}{dq^2 d\cos\theta_l} d\cos\theta_l\right) / \Gamma_{tot}. \tag{17}$$

The ratio of differential branching ratio can be written as:

$$R(q^2) = \frac{DBR(q^2)(\Xi_b \to \Xi_c \tau \bar{\nu}_\tau)}{DBR(q^2)(\Xi_b \to \Xi_c l \bar{\nu}_l)}. \tag{18}$$

Other q^2 dependent observables such as $A_{FB}(q^2)$, $P_{\Xi_c}(q^2)$, $P_\tau(q^2)$ and $C_F(q^2)$ have the formalisms as:

$$\begin{aligned}
A_{FB}(q^2) &= \frac{\int_0^1 \frac{d\Gamma}{dq^2 d\cos\theta_l} d\cos\theta_l - \int_{-1}^0 \frac{d\Gamma}{dq^2 d\cos\theta_l} d\cos\theta_l}{\int_0^1 \frac{d\Gamma}{dq^2 d\cos\theta_l} d\cos\theta_l + \int_{-1}^0 \frac{d\Gamma}{dq^2 d\cos\theta_l} d\cos\theta_l}, \\
P_{\Xi_c}(q^2) &= \frac{d\Gamma^{\lambda_2=1/2}/dq^2 - d\Gamma^{\lambda_2=-1/2}/dq^2}{d\Gamma^{\lambda_2=1/2}/dq^2 + d\Gamma^{\lambda_2=-1/2}/dq^2}, \\
P_\tau(q^2) &= \frac{d\Gamma^{\lambda_\tau=1/2}/dq^2 - d\Gamma^{\lambda_\tau=-1/2}/dq^2}{d\Gamma^{\lambda_\tau=1/2}/dq^2 + d\Gamma^{\lambda_\tau=-1/2}/dq^2}, \\
C_F(q^2) &= \frac{1}{\mathcal{H}_{tot}} \frac{d^2 W(\theta_l)}{d(\cos\theta_l)^2}, \quad \mathcal{H}_{tot} = \int W(\theta_l) d\cos\theta_l, \quad W(\theta_l) = A_1 + \frac{m_l^2}{q^2} A_2, \\
\frac{d^2 W(\theta_l)}{d(\cos\theta_l)^2} &= \frac{3}{4}\left(1 - \frac{m_l^2}{q^2}\right)\left[H_{1/2,1}^2 + H_{-1/2,-1}^2 - 2(H_{1/2,0}^2 + H_{-1/2,0}^2)\right],
\end{aligned} \tag{19}$$

where $d\Gamma^{\lambda_\tau=1/2}/dq^2$ and $d\Gamma^{\lambda_\tau=-1/2}/dq^2$ represent the differential branching ratio of positive and negative helicity for τ lepton as well as $d\Gamma^{\lambda_2=1/2}/dq^2$ and $d\Gamma^{\lambda_2=-1/2}/dq^2$ are the same meaning for Ξ_c baryon. The detail formalism of them can be found in Ref. [18].

4. Numerical results and discussions

In this section, we study the NP contributions of vector LQ to the aforementioned observables which may produce deviations from the corresponding SM predictions at high level. To obtain numerical results, we first present all the inputs relevant to our calculation in Table 1. For the form factors, we use the results from relativistic quark model calculated by Ref. [26]. The relevant parameters for the form factors are given in Table 2. We consider the uncertainty of NP parameters (within 1σ range of the central values), form factors (10% of the central values) and V_{cb} (10% of the central values) when we calculate all the observables for $\Xi_b \to \Xi_c \tau \bar{\nu}_\tau$ decay. The mass of LQ is taken as $M_U = 1$ TeV. Now we show our predictions for the several observables both in SM and vector LQ scenarios by figures. In Fig. 1(a)–(c), we display the predictions in SM and vector LQ scenarios for the q^2 dependences of $DBR(q^2)$, the ratio $R_{\Xi_c}(q^2)$ and $C_F(q^2)$, respectively. In Fig. 1(a), the gray band represents the SM predictions for $DBR(q^2)$ whereas the lightblue band and red band represent the contributions of vector LQ to $DBR(q^2)$

Table 1
Input parameters of SM used in our numerical analysis [39].

$m_b(m_b) = 4.18$ GeV	$m_c(m_c) = 1.28$ GeV
$m_1 = 5.7919$ GeV	$m_2 = 2.46787$ GeV
$\tau_{\Xi_b} = 1.479 \times 10^{-12}$ s	$\lvert V_{cb}\rvert = 0.0409$
$m_e = 0.510998928 \times 10^{-3}$ GeV	$m_\mu = 0.10565$ GeV
$G_F = 1.166378 \times 10^{-5}$ GeV^{-2}	$m_\tau = 1.77682$ GeV

Table 2
Parameters of form factors for $\Xi_b \to \Xi_c \tau \bar{\nu}_\tau$ decay.

$\bar{\Lambda}$ GeV	ρ_ζ^2	c_ζ	ρ_χ^2	c_χ
0.970	2.27	3.87	0.045	0.036

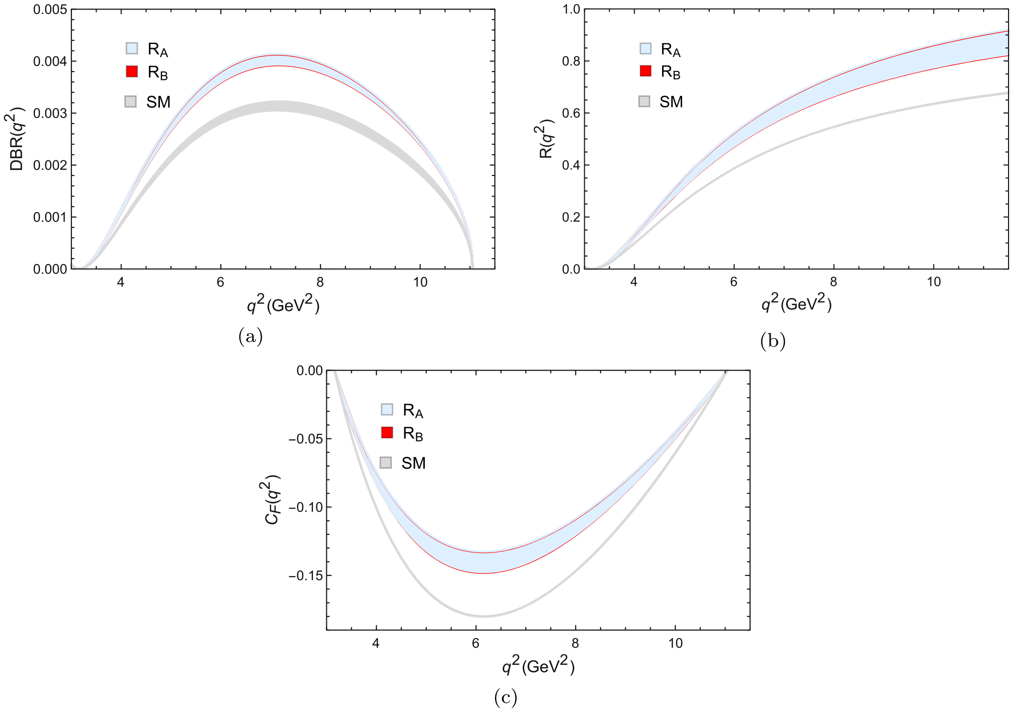

Fig. 1. q^2 dependence of observables $DBR(q^2)$ (a), $R_{\Xi_c}(q^2)$ (b) and $C_F(q^2)$ (c) within SM and vector LQ scenario. The uncertainty of form factors, V_{cb} and NP parameters are all included. (For interpretation of the colours in the figure(s), the reader is referred to the web version of this article.)

in R_A and R_B cases, respectively. We can see that the effects of vector LQ to the observable $DBR(q^2)$ is prominent and induce large deviation from the SM predictions. Comparing to the SM predictions, the values of $DBR(q^2)$ are enhanced by about 28% both in R_A and R_B cases for all the reasonable q^2. Another Obvious feature is that the lightblue band and red band are nearly complete overlapped, because of the approximate results given by R_A and R_B cases. In order to comprehend this, we should notice that there is only (V–A) couplings in vector LQ contributions and corresponding to the best-fit solutions R_A and R_B cases, the numerical results of effective coefficients C_V and C_A are given, respectively, as:

$$C_V = C_A = \begin{cases} 1.133 \pm 0.030 & R_A \\ -1.135 \pm 0.030 & R_B, \end{cases}$$

we can obtain that C_V and C_A have almost the same absolute values for the two solutions R_A and R_B. In Fig. 1(b), similarly, the gray line represents the SM predictions for $R_{\Xi_c}(q^2)$ whereas the lightblue band and red band represent the contributions of vector LQ to the ratio $R_{\Xi_c}(q^2)$ in R_A and R_B cases, respectively. Different from the contributions of vector LQ to the $DBR(q^2)$, the numerical results of $R_{\Xi_c}(q^2)$ are the rising trend with the increasing q^2. The lightblue band and red band are also overlapped due to the same essence of two solutions R_A and R_B. We also see that the effects of vector LQ to the ratio $R_{\Xi_c}(q^2)$ is apparent and have large deviation from the SM predictions. We hope this observable will be detected on the high energy collider in the future which may also again pronounce the sign of NP. The numerical results of SM and vector LQ contributions to observable $C_F(q^2)$ are displayed in Fig. 1(c). The line and bands have the same meaning as that in Fig. 1(b). The numerical results of $C_F(q^2)$ are also sensitive to the contributions of vector LQ which show large deviation from the SM predictions. The numerical results of $C_F(q^2)$ can be enhanced by about 22% in both R_A and R_B cases for all the reasonable q^2 spectra. The values of $C_F(q^2)$ are all under zero which agree with the results of them in Ref. [32]. It is worthwhile to note that the observable $C_F(q^2)$ is only dependent of the new vector couplings [17], but not of other scalar couplings. Thus, once experimental measurement of this observable is achieved, the NP effects coming from vector type of interactions will be verified which can distinguish between the vector and scalar type of interactions. In conclusion, the observables $DBR(q^2)$, $R_{\Xi_c}(q^2)$ and $C_F(q^2)$ are all sensitive to the NP effects of vector LQ. We hope that if they are observed on high energy collider in the future, our theory analysis will provide guidance and evidence for discriminating the possible NP signal.

The contributions of SM and vector LQ to q^2 dependences of $A_{FB}(q^2)$, $P_{\Xi_c}(q^2)$ and $P_\tau(q^2)$ are displayed in Fig. 2(a)–(c), correspondingly. We can see that these observables possess one common feature, i.e., the numerical results in SM or vector LQ scenario are the same. The every only line in Fig. 2(a)–(c) dedicates the contributions coming from either SM or vector LQ scenario. Because the NP effects of vector LQ are eliminated exclusively for the sake of effective coefficient C_V and C_A of (V–A) couplings appearing both in the numerator and denominator of these ratios. In Fig. 2(a), we can see that the numerical results of $A_{FB}(q^2)$ increase with the increasing of q^2 and achieve the maximum at $q^2 \sim 10\ \text{GeV}^2$. The rising tendency of numerical results of $P_{\Xi_c}(q^2)$ with the increasing of q^2 are shown in Fig. 2(c), whereas $P_\tau(q^2)$ have descendent tendency with the increasing of q^2 in Fig. 2(b). There are a zero crossing both in the numerical results of $A_{FB}(q^2)$ and $P_\tau(q^2)$. In conclusion, all these three observables are insensitive to the contributions of vector LQ and have nearly the same behaviour as that in the SM.

5. Summary and conclusion

The deviations of $R_D^{(*)}$, $R_K^{(*)}$ and $R_{J/\Psi}$ between the experimental measurements and corresponding SM predictions indicate the lepton flavor universality violation. These anomalies may reveal the existence of NP. It is necessary to further explore the NP effects of these B meson decay anomalies. We choose the baryon semileptonic decay $\Xi_b \to \Xi_c \tau \bar{\nu}_\tau$ as the target object. This is because on one hand, study of $\Xi_b \to \Xi_c \tau \bar{\nu}_\tau$ decay may provide new viewpoints to comprehend $R_D^{(*)}$ anomalies and be the continuity of NP signal. On the other hand, it is useful to

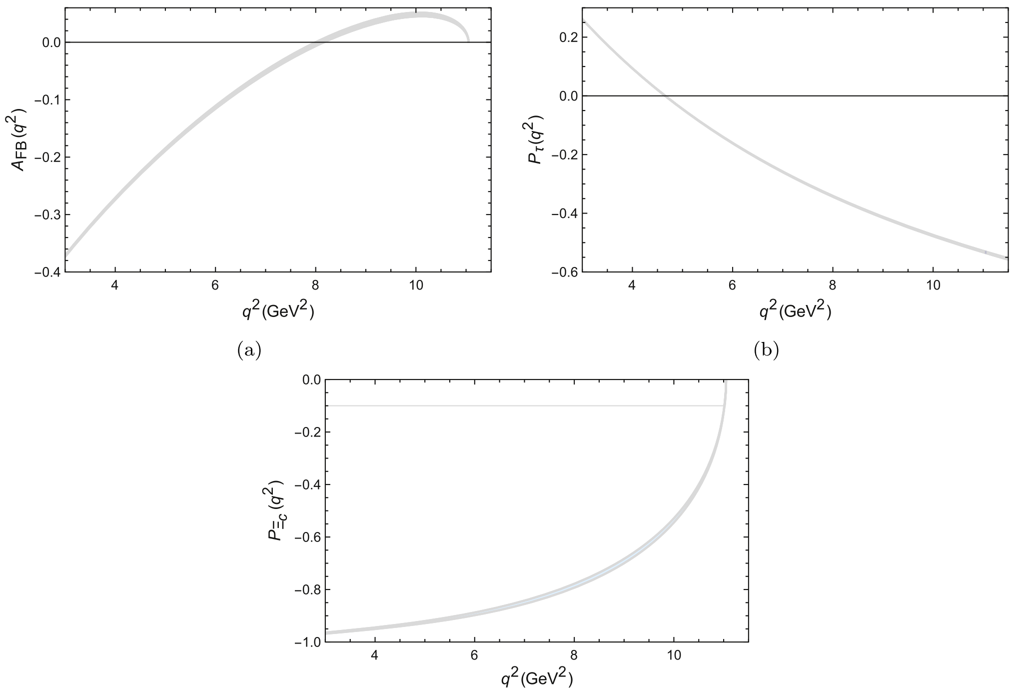

(a) (b) (c)

Fig. 2. q^2 dependence of observables $A_{FB}(q^2)$ (a), $P_\tau(q^2)$ (b) and $P_{\Xi_c}(q^2)$ (c) within SM and vector LQ scenarios. The only band in (a)–(c) represents the contributions of SM or vector LQ scenario. The uncertainty of form factors, V_{cb} and NP parameters are all included.

precise calculation of the main ingredients of SM such as CKM matrix and exploring the nature of CP violation. The SM with a single vector LQ $U_3(3, 3, \frac{2}{3})$ can resolve the $R_D^{(*)}$ anomalies which have been verified by Ref. [14]. In order to further explore the NP effects of $R_D^{(*)}$ anomalies, in this paper, we investigate the NP effects of vector LQ $U_3(3, 3, \frac{2}{3})$ to baryon semileptonic $\Xi_b \to \Xi_c \tau \bar{\nu}_\tau$ decay.

Using the helicity amplitude formalism and the form factors resulted from relativistic quark model, we discuss the observables such as differential branching ratio $DBR(q^2)$, ratio of differential branching ratio $R_{\Xi_c}(q^2)$, lepton-side forward-backward asymmetry $A_{FB}(q^2)$, longitudinal polarization fraction of Ξ_c baryon $P_{\Xi_c}(q^2)$ and τ lepton $P_\tau(q^2)$ as well as the convexity parameter $C_F(q^2)$ behaving as the functions of q^2 in SM as well as R_A and R_B cases of vector LQ scenarios. The numerical results of these observables are reported in SM as well as two best-fit solutions R_A and R_B of vector LQ scenario which have been shown in Fig. 1 and Fig. 2. The numerical results of the observables $DBR(q^2)$, $R_{\Xi_c}(q^2)$ and $C_F(q^2)$ in Fig. 1(a)–(c) display that they are sensitive to the NP effects of vector LQ and have significant deviations from their corresponding SM predictions. R_A and R_B cases of vector LQ scenario have nearly the same results (the lightblue and red bands are almost overlapped) because the identical essence of them. In all the acceptable q^2 spectra, the numerical results of $DBR(q^2)$ can be enhanced by about 28% in both R_A and R_B cases, nevertheless, the numerical results of $C_F(q^2)$ can be enhanced by about 22% in both R_A and R_B cases within all the reasonable q^2 spectra. If NP exist, the ratio $R_{\Xi_c}(q^2)$ may have the same character with $R_D^{(*)}$. We hope that the precise measurement of it will give new viewpoints to the comprehension of $R_D^{(*)}$ anomalies and our analysis will provide the theory guidance for experimental searching. The observable $C_F(q^2)$ is useful for distinguishing the NP effects coming from vector or scalar type interactions. As a conclusion, the contributions of vector LQ to the observables $DBR(q^2)$, $R_{\Xi_c}(q^2)$ and $C_F(q^2)$ are prominent and we hope they will be measured on high energy collider in the future. The numerical results of observables $A_{FB}(q^2)$, $P_\tau(q^2)$ and $P_{\Xi_c}(q^2)$ in Fig. 2(a)–(c) is not sensitive to the NP effects of vector LQ because the Wilson coefficients affected by the NP contributions of vector LQ appear both in numerator and denominator. In this case, the NP effects are cancelled and these three observables have the same behaviour of that in the SM.

Even though there is no direct evidence for existence of NP, both theoretical and experimental researches of baryon $\Xi_b \to \Xi_c \tau \bar{\nu}_\tau$ decay are important for the sake of outstanding $R_D^{(*)}$ and $R_{J/\Psi}$ anomalies. If the experimental measurements of the observables $DBR(q^2)$, $R_{\Xi_c}(q^2)$ and $C_F(q^2)$ have deviations from their corresponding SM predictions, we can consider that this follows the step of NP effects accompanying with $R_D^{(*)}$ and $R_{J/\Psi}$ anomalies as well as further verifies the existence of NP. Additional, more precise measurement of the branching ratio of $\Xi_b \to \Xi_c l \bar{\nu}_l$ decay and more precise calculation of the form factors for $\Xi_b \to \Xi_c$ may determinate the CKM matrix element $|V_{cb}|$ more accurately.

Acknowledgements

This work was supported by the National Natural Science Foundation of China under Grants Nos. 11547266 and 11605110; the Natural Science Foundation of Henan Province Grant Nos. 16A140045, 152102210330, 17A430004 and 16A140012.

References

[1] J.P. Lees, et al., BaBar Collaboration, Phys. Rev. Lett. 109 (2012) 101802, arXiv:1205.5442 [hep-ex].
[2] J.P. Lees, et al., BaBar Collaboration, Phys. Rev. D 88 (7) (2013) 072012, arXiv:1303.0571 [hep-ex].
[3] M. Huschle, et al., Belle Collaboration, Phys. Rev. D 92 (7) (2015) 072014, arXiv:1507.03233 [hep-ex].
[4] A. Abdesselam, et al., Belle Collaboration, arXiv:1603.06711 [hep-ex].
[5] A. Abdesselam, et al., Belle Collaboration, arXiv:1608.06391 [hep-ex].
[6] R. Aaij, et al., LHCb Collaboration, Phys. Rev. Lett. 115 (11) (2015) 111803, arXiv:1506.08614 [hep-ex]; Erratum: Phys. Rev. Lett. 115 (15) (2015) 159901.
[7] R. Aaij, et al., LHCb Collaboration, Phys. Rev. Lett. 120 (17) (2018) 171802, arXiv:1708.08856 [hep-ex].
[8] Heavy Flavor Averaging Group Collaboration, http://www.slac.stanford.edu/xorg/hfag/semi/fpcp17/RDRDs.html.
[9] R. Aaij, et al., LHCb Collaboration, Phys. Rev. Lett. 113 (2014) 151601, arXiv:1406.6482 [hep-ex].
[10] R. Aaij, et al., LHCb Collaboration, J. High Energy Phys. 1708 (2017) 055, https://doi.org/10.1007/JHEP08(2017)055, arXiv:1705.05802 [hep-ex].
[11] R. Aaij, et al., LHCb Collaboration, Phys. Rev. Lett. 120 (12) (2018) 121801, arXiv:1711.05623 [hep-ex].
[12] W.F. Wang, Y.Y. Fan, Z.J. Xiao, Chin. Phys. C 37 (2013) 093102, arXiv:1212.5903 [hep-ph].
[13] R. Dutta, A. Bhol, Phys. Rev. D 96 (7) (2017) 076001, arXiv:1701.08598 [hep-ph].
[14] S. Fajfer, N. Košnik, Phys. Lett. B 755 (2016) 270, arXiv:1511.06024 [hep-ph].
[15] M. Freytsis, Z. Ligeti, J.T. Ruderman, Phys. Rev. D 92 (5) (2015) 054018, arXiv:1506.08896 [hep-ph].
[16] A. Celis, M. Jung, X.Q. Li, A. Pich, Phys. Lett. B 771 (2017) 168, arXiv:1612.07757 [hep-ph].
[17] R. Dutta, Phys. Rev. D 93 (5) (2016) 054003, arXiv:1512.04034 [hep-ph].
[18] X.Q. Li, Y.D. Yang, X. Zhang, J. High Energy Phys. 1702 (2017) 068, arXiv:1611.01635 [hep-ph].
[19] R.N. Faustov, V.O. Galkin, Phys. Rev. D 94 (7) (2016) 073008, arXiv:1609.00199 [hep-ph].
[20] T. Gutsche, M.A. Ivanov, J.G. Körner, V.E. Lyubovitskij, P. Santorelli, N. Habyl, Phys. Rev. D 91 (7) (2015) 074001, arXiv:1502.04864 [hep-ph]; Erratum: Phys. Rev. D 91 (11) (2015) 119907.

[21] S. Shivashankara, W. Wu, A. Datta, Phys. Rev. D 91 (11) (2015) 115003, https://doi.org/10.1103/PhysRevD.91.115003, arXiv:1502.07230 [hep-ph].
[22] R. Watanabe, arXiv:1709.08644 [hep-ph].
[23] B. Chauhan, B. Kindra, arXiv:1709.09989 [hep-ph].
[24] B. Wei, J. Zhu, J.H. Shen, R.M. Wang, G.R. Lu, arXiv:1801.00917 [hep-ph].
[25] K. Azizi, Y. Sarac, H. Sundu, Eur. Phys. J. A 48 (2012) 2, arXiv:1107.5925 [hep-ph].
[26] D. Ebert, R.N. Faustov, V.O. Galkin, Phys. Rev. D 73 (2006) 094002, arXiv:hep-ph/0604017.
[27] R.L. Singleton, Phys. Rev. D 43 (1991) 2939.
[28] M.A. Ivanov, V.E. Lyubovitskij, J.G. Korner, P. Kroll, Phys. Rev. D 56 (1997) 348, arXiv:hep-ph/9612463.
[29] M.A. Ivanov, J.G. Korner, V.E. Lyubovitskij, A.G. Rusetsky, Phys. Rev. D 59 (1999) 074016, arXiv:hep-ph/9809254.
[30] C. Albertus, E. Hernandez, J. Nieves, Phys. Rev. D 71 (2005) 014012, arXiv:nucl-th/0412006.
[31] J.G. Korner, M. Kramer, D. Pirjol, Prog. Part. Nucl. Phys. 33 (1994) 787, arXiv:hep-ph/9406359.
[32] R. Dutta, Phys. Rev. D 97 (7) (2018) 073004, arXiv:1801.02007 [hep-ph].
[33] K. Azizi, A.T. Olgun, Z. Tavukoglu, Adv. High Energy Phys. 2017 (2017) 7435876, https://doi.org/10.1155/2017/7435876, arXiv:1609.09678 [hep-ph].
[34] S. Chatrchyan, et al., CMS Collaboration, Phys. Rev. Lett. 110 (8) (2013) 081801.
[35] A.M. Sirunyan, et al., CMS Collaboration, J. High Energy Phys. 1807 (2018) 115.
[36] M. Aaboud, et al., ATLAS Collaboration, Phys. Rev. Lett. 120 (16) (2018) 161802, https://doi.org/10.1103/PhysRevLett.120.161802, arXiv:1801.06992 [hep-ex].
[37] V. Khachatryan, et al., CMS Collaboration, Phys. Lett. B 755 (2016) 196, https://doi.org/10.1016/j.physletb.2016.02.002, arXiv:1508.04308 [hep-ex].
[38] M. Abdullah, J. Calle, B. Dutta, A. Flórez, D. Restrepo, Phys. Rev. D 98 (5) (2018) 055016, https://doi.org/10.1103/PhysRevD.98.055016, arXiv:1805.01869 [hep-ph].
[39] C. Patrignani, et al., Particle Data Group, Chin. Phys. C 40 (10) (2016) 100001.